Carbohydrate Polymers 368 (2025) 124095

Contents lists available at ScienceDirect

Carbohydrate Polymers

journal homepage: www.elsevier.com/locate/carbpol

Conformational and rheological behavior of kappa carrageenan in glycerol: Effects of sodium salts and preparation temperature

Mihail T. Georgiev [a,d,*], Silviya S. Simeonova [b], Boris G. Konstantinov [a], Krassimir D. Danov [a,d], Robert Riley [c], Dawn Woodall [c]

[a] Department of Chemical and Pharmaceutical Engineering, Faculty of Chemistry and Pharmacy, Sofia University, Sofia 1164, Bulgaria
[b] Department of Physical Chemistry, Faculty of Chemistry and Pharmacy, University of Sofia, Sofia 1164, Bulgaria
[c] Unilever Research & Development Port Sunlight, Bebington CH63 3JW, UK
[d] CoC "Smart Mechatronics, Eco- and Energy Saving Systems and Technologies", Sofia 1164, Bulgaria

ARTICLE INFO

Keywords:
Kappa carrageenan
Rheology
AFM
Glycerol
Sodium salts
Helix-to-coil transition

ABSTRACT

Kappa carrageenan (KC), a sulfated polysaccharide derived from red seaweed, exhibits distinct gelation properties that are influenced by ionic strength and thermal conditions. While its behavior in aqueous media is well-established, understanding KC's gelation mechanisms in non-aqueous solvents (like glycerol) remains limited. This study investigates the conformational and rheological properties of kappa carrageenan in glycerol, focusing on the effects of sodium salts (NaCl, NaH_2PO_4, Na_3PO_4) at varying concentrations and preparation temperatures (60 °C and 80 °C). Rheological measurements reveal distinct viscosity trends influenced by salt type and temperature, highlighting the interplay between ionic interactions and KC's conformational transitions. Phosphate salts significantly enhance network elasticity and stability, especially at intermediate concentrations, whereas NaCl induces weaker, viscosity-dominated structures. Atomic force microscopy imaging provides complementary nanoscale insights, showcasing salt-specific structural transitions from looped to branched networks, alongside a temperature-dependent helix-to-coil transformation. These results illustrate how the precisely tuning ionic conditions and the preparation temperatures in glycerol media can effectively modulate KC's structure and viscoelastic properties. This deeper understanding facilitates targeted design and optimization of carrageenan-based materials across food, pharmaceutical, cosmetic, and biotechnological applications.

1. Introduction

Kappa carrageenan, a sulfated polysaccharide derived from red seaweed, is renowned for its gelation properties, making it a valuable component in various industrial applications, including food, pharmaceuticals, and cosmetics (Rupert et al., 2022). KC's unique ability to form gels is highly dependent on environmental conditions such as ionic strength and temperature, as well as its interactions with counterions (Brenner et al., 2014; Tako, 2015).

The gelation mechanism of kappa carrageenan involves a two-step process: helix formation on cooling and subsequent aggregation of helices into a network structure (Geonzon et al., 2019; Hermansson, 1989). This process is significantly influenced by the presence of specific cations, which can induce or inhibit gel formation depending on their size and charge (Mangione et al., 2005; Watase et al., 1990). Sodium salts (NaCl, NaH_2PO_4, and Na_3PO_4) play a critical role in this mechanism by providing varying ionic strengths and pH environments, thus affecting the structural dynamics and the final gels' properties (Ciancia et al., 1997; Derkach et al., 2018).

The lower dielectric constant of glycerol compared to water creates unique gelation conditions for kappa carrageenan, influencing the electrostatic interactions and the network dynamics (Ramakrishnan & Prud'homme, 2000a). The lower dielectric constant affects the electrostatic interactions between kappa carrageenan molecules and the added salts, thereby altering the gelation kinetics and the final gel properties (Ramakrishnan & Prud'homme, 2000b; Ramm et al., 2021). Additionally, glycerol can prevent the chemical degradation and enhance the stability of biopolymers by modifying the respective system parameters such as the viscosity and the elasticity (Stenner et al., 2016).

Temperature is another crucial factor influencing the gelation process (Mangione et al., 2003). Elevated temperatures enhance the dissolution of the polysaccharide and the ions' mobility, facilitating

* Corresponding author at: Department of Chemical and Pharmaceutical Engineering, Faculty of Chemistry and Pharmacy, Sofia University, Sofia 1164, Bulgaria.
E-mail address: mtg@lcpe.uni-sofia.bg (M.T. Georgiev).

https://doi.org/10.1016/j.carbpol.2025.124095
Received 23 April 2025; Received in revised form 16 July 2025; Accepted 18 July 2025
Available online 19 July 2025

more efficient gel formation (Hjerde et al., 1999). However, careful temperature control is essential to prevent the degradation of kappa carrageenan and to maintain the integrity of the gel network (Ikeda et al., 2001). Different aggregation mechanisms of kappa carrageenan in diverse solvents have been observed, indicating distinct network formations in water compared to more randomized structures in glycerol and sorbitol (Cao & Mezzenga, 2020; Diener et al., 2019).

Our investigation explores the self-assembly processes of kappa carrageenan in a glycerol medium building on the foundation of previous studies. Specifically, it examines the effects of different Na^+ ion sources (NaCl, NaH_2PO_4, Na_3PO_4) under varied stirring temperatures (60 °C and 80 °C). The rheological measurements provide insights into the mechanical properties and the viscoelastic behavior of the formed gels, while the atomic force microscopy (AFM) offers a detailed view of the microstructural changes and network formation at the nanoscale (Funami et al., 2007; Schefer et al., 2014).

The interaction of KC with large-site univalent cations such as K^+, Rb^+, and Cs^+ significantly alters its rheological behavior compared to smaller Na^+ ions (Ciancia et al., 1997; Diener et al., 2019; Schefer et al., 2015; Thrimawithana et al., 2010). The considerable differences are attributed to the steric capabilities of these cations to engage in the ionic and electrostatic attractions, thus influencing the gel properties and stability (Bui et al., 2019). The previous studies have examined also the impact of uniform ions, specifically ammonium salts, on the rheological and thermal properties of kappa carrageenan gels, highlighting the effects of a consistent ion while varying the coion (Watase et al., 1990). Although ammonium ions were used in these studies, our research adopts a similar methodology by fixing the counterion and varying the coion. While Na^+ is not the most effective structuring ion for kappa carrageenan, investigating different Na^+ sources offer valuable insight into how coion identity influences gelation in non-aqueous media. Glycerol is widely used in food, cosmetic, and pharmaceutical formulations, yet the structural behavior of carrageenans in such media remains poorly understood. This work addresses this gap by systematically examining the influence of NaCl, NaH_2PO_4, and Na_3PO_4 on the conformational and rheological properties of kappa carrageenan in glycerol, under different preparation temperatures. The combination of rheological characterization with AFM visualization enables to obtain correlations of the ion-specific effects with the nanoscale structure, offering both mechanistic insight and practical guidance for formulation design.

This study tests the hypothesis that both coion identity and preparation temperature critically influence the helix–coil transitions and network formation of kappa carrageenan in glycerol. It is proposed that specific sodium salts (NaCl, NaH_2PO_4, Na_3PO_4), through their coion effects, modulate intramolecular and intermolecular interactions, thereby altering viscoelastic properties and nanoscale morphology.

2. Materials and methods

2.1. Materials

Commercially available kappa carrageenan (GENU® SMART 118; CP Kelco) was used as received. Elemental analysis by atomic flame spectroscopy (0.1 % *w/v* solution) showed concentrations of Na^+: 3.7 mg/L (0.161 mM), K^+: 41 mg/L (1.048 mM), and Ca^{2+}: 4.2 mg/L (0.105 mM). X-ray fluorescence (XRF) analysis using a Bruker S1 TITAN handheld spectrometer determined the sulfur content to be 7.4 % by mass, corresponding to approximately 0.91 sulfate groups per disaccharide unit. The residual K^+ corresponds to ~0.83 mol per disaccharide unit and is present equally in all samples. To account for its structural effects, reference samples without added sodium salts were included. These K^+-only systems serve as internal controls, as shown in the NaCl results section.

(3-Aminopropyl) triethoxysilane (APTES, CAS 919–30-2, 99.9 % purity) for mica modification, and Sodium phosphate (CAS: 7558-80-7; ≥99.0 % purity, anhydrous) were obtained from Sigma-Aldrich. Trisodium phosphate (CAS: 7601-54-9, ≥98.0 % purity) was sourced from Sigma-Aldrich. Muscovite mica discs type V-1 were purchased from NanoandMore GMBH. Deionized water, with a resistivity of 15.0 MΩ·cm at 25 °C, was produced using a Millipore Elix water purification system.

2.2. Solution preparation and experimental setup

For rheological measurements the KC stock solutions were prepared at 0.5 wt% KC in glycerol with added sodium salts spanning 0–670 mM absolute concentration. All salt concentrations reported in the manuscript therefore refer to this total salt content at the fixed polymer level of 0.5 wt%.

For AFM analysis each stock was subsequently diluted five-fold with glycerol, giving 0.1 wt% KC while maintaining the original KC-to-salt ratio. This step lowers viscosity enough for reliable imaging but preserves the local ionic environment experienced by the polymer chains.

Glycerol was pre-heated to either 60 °C or 80 °C, after which KC powder was gradually dispersed under vigorous stirring (4000 rpm) with a Silverson high-shear mixer fitted with a general-purpose disintegrating head. Continuous mixing for 1 h prevented clumping and ensured homogeneous hydration while the vessel sat in a thermostatted water bath. The appropriate amount of sodium salt was then added to reach the target absolute concentration (0–670 mM in the 0.5 wt% stock), and stirring continued for a further 15 min at the selected temperature. Samples were left to equilibrate overnight at room temperature before rheological testing or dilution for AFM.

The selected salt concentration range - from 0 mM (no added salt) to 670 mM—was designed to cover a broad range of polymer-to-salt ratios typically encountered in industrial formulations. This range allows us to capture the transition from low-ionic-strength conditions, where minimal structural reorganization occurs, to high-salt regimes that strongly influence carrageenan network assembly.

The pH of the samples after equilibration varied with the added salt: ~8.0 for kappa carrageenan in glycerol alone, ~5.5 with NaCl, ~6.0 with NaH_2PO_4, and ~ 11.2 with Na_3PO_4. These values reflect the intrinsic pH of the salts in glycerol. However, since sulfate groups in carrageenan remain ionized across this pH range, the variations in viscoelastic behavior and network morphology are attributed to the specific ion and coion effects rather than pH-induced changes in carrageenan protonation or chain conformation.

2.3. AFM sample preparation and imaging

The mica surface was modified using APTES, following a procedure adapted from Schefer et al., 2014, with a spin-assisted cleaning step introduced to improve the carrageenan immobilization in viscous glycerol-based solutions. Freshly cleaved muscovite mica (V-1 grade) was placed in a closed glass desiccator with 50 μL of APTES and exposed to vapor-phase silanization for 2 h at room temperature. This treatment yields a positively charged mica surface that promotes electrostatic binding of the negatively charged carrageenan chains.

AFM samples were prepared one day after solution mixing, following overnight equilibration at room temperature. For imaging, the carrageenan solutions were diluted fivefold (to 0.1 wt%) while preserving the original carrageenan-to-salt ratio. A 20 μL aliquot of the diluted solution was deposited onto the modified mica for 1 min to allow immobilization of the carrageenan segments. Due to the viscosity of glycerol, excess material was then removed by spin-coating the sample at 4000 rpm for 5 min, leaving only the immobilized carrageenan structures on the surface.

AFM imaging was performed using a MultiMode V system (Bruker Ltd., Germany) in tapping mode under ambient conditions. Commercial silicon nitride cantilevers (Tap150-G) were used to scan 2 × 2 μm areas at 512 × 512 pixel resolution. Height measurements were extracted with a standard deviation of ±0.1 nm.

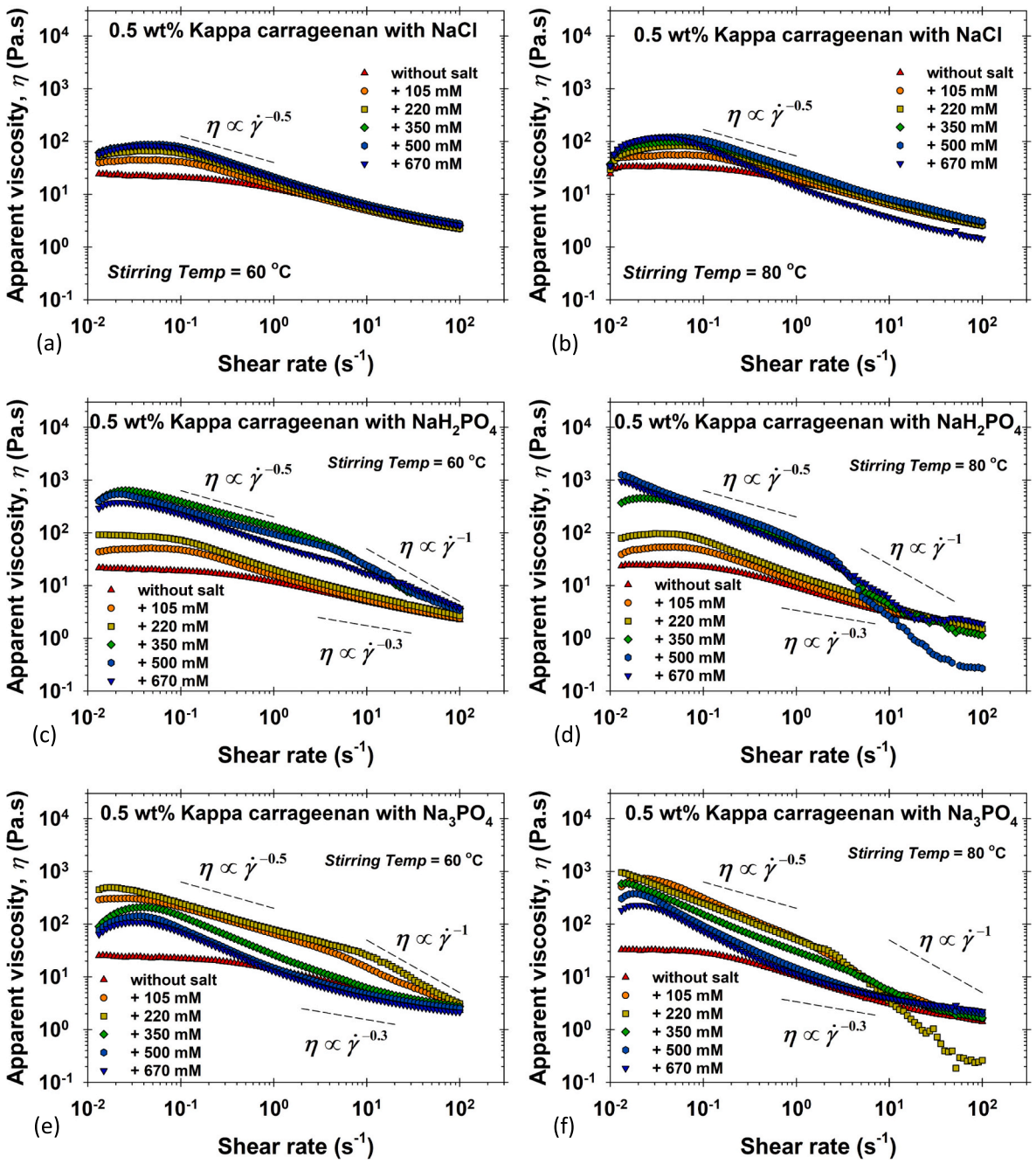

Fig. 1. Rheological analysis of 0.5 wt% kappa carrageenan solutions with varying concentrations of sodium salts measured at 25 °C. Panels (a) and (b) display the apparent viscosity, η, of kappa carrageenan solutions with NaCl at stirring temperature of 60 °C and 80 °C, respectively. Panels (c) and (d) show the viscosity profiles with NaH_2PO_4 at the same temperatures. Panels (e) and (f) depict the effects of Na_3PO_4 under identical conditions. Each graph illustrates the viscosity across a shear rate range of 0.01 to 100 s^{-1}, highlighting shear-thinning behavior. The power-law relationships are noted for different salts, with $\eta \propto \dot{\gamma}^{-0.5}$ commonly observed, though some samples with phosphate salts exhibit deviations (from $\eta \propto \dot{\gamma}^{-0.3}$ to $\eta \propto \dot{\gamma}^{-1}$), indicating altered network dynamics. The data points are represented by symbols corresponding to varying salt concentrations from 105 mM to 670 mM, elucidating the influence of the ionic strength and ion type on the rheological behavior of the solutions.

2.4. Rheological measurements

The rheological properties of the KC solutions were measured using Gemini rotational rheometer (Malvern Instruments, UK) equipped with a cone-and-plate geometry (diameter: 40 mm; cone angle: 4°). The measurements were conducted at a controlled temperature of 25 ± 0.1 °C maintained by a Peltier temperature control system. For viscosity measurements, steady shear rate sweeps were performed in the shear rate range from 0.01 to 100 s^{-1}, using a logarithmic profile with approximately 25 data points per decade. The rheometer automatically adjusted the acquisition time at each point to ensure steady-state conditions, based on a torque stability criterion of 1 % deviation. The elastic properties were assessed through oscillatory rheological measurements. Amplitude sweeps at a constant frequency of 1 Hz were initially conducted to determine the linear viscoelastic region (LVER). Frequency sweeps within the determined LVER were subsequently performed from 0.1 to 100 Hz to measure the storage (G') and loss (G'') moduli.

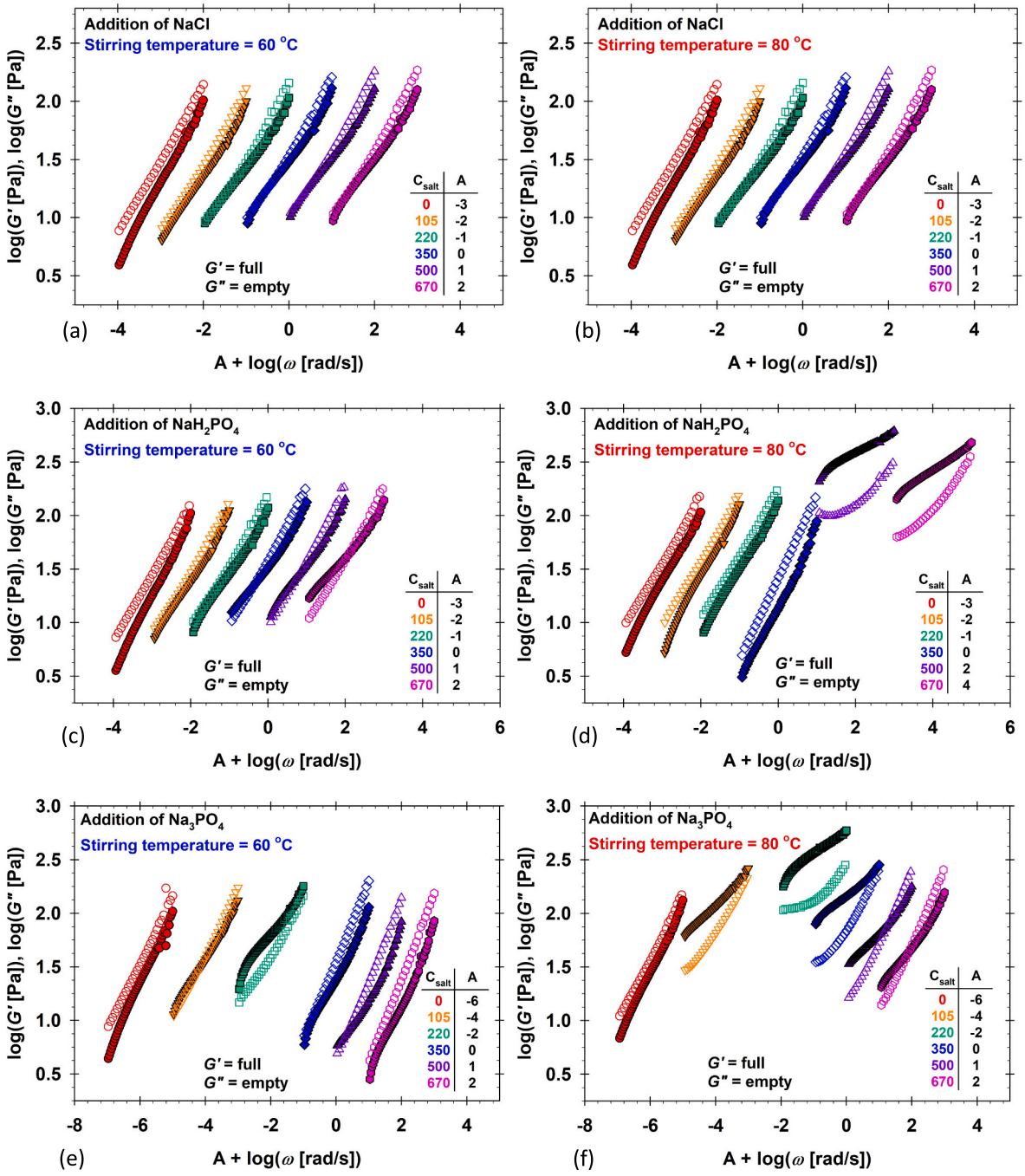

Fig. 2. Frequency-dependent viscoelastic behavior (*G*', *G*") of kappa carrageenan solutions prepared with varying sodium salts (NaCl, NaH_2PO_4, Na_3PO_4) at stirring temperatures of 60 °C (blue) and 80 °C (red). Panels (a) and (b) show the effects of NaCl at different salt concentrations (0–670 mM); panels (c) and (d) illustrate the behavior with NaH_2PO_4, and panels (e) and (f) represent Na_3PO_4. Solid symbols denote the storage modulus (*G*'), while open symbols denote the loss modulus (*G*"). The log-log plots highlight the influence of salt type, ionic strength, and temperature on the viscoelastic properties, demonstrating enhanced gel elasticity (G') at intermediate concentrations for phosphate salts and more balanced viscoelasticity for NaCl. The curves were shifted sideways (factor A) to avoid overlap. (For interpretation of the references to colour in this figure legend, the reader is referred to the web version of this article.)

3. Results

3.1. Rheological behavior of kappa carrageenan solutions

3.1.1. Apparent viscosity

The apparent viscosity of KC solutions measured at 25 °C showed a marked dependence on both the stirring temperature (60 °C vs. 80 °C) and the type of sodium salt used. These temperatures were selected to fall below and above the known helix–coil transition of KC in glycerol (Ramakrishnan & Prud'homme, 2000b). At 60 °C, KC chains are partially helical, while at 80 °C, they adopt a disordered coil state. This conformational difference governs how salts influence the network formation during cooling.

For phosphate salts (NaH_2PO_4 and Na_3PO_4), samples prepared at 60 °C generally exhibited higher viscosities than those prepared at 80 °C (Fig. 1). This reflects the preservation of helical structure and the formation of partially ordered networks during cooling. In contrast, preparation at 80 °C promotes the helix-to-coil transition and the greater chain flexibility. For studied phosphate systems, the increased flexibility appears to enhance the chain entanglement and the junction formation

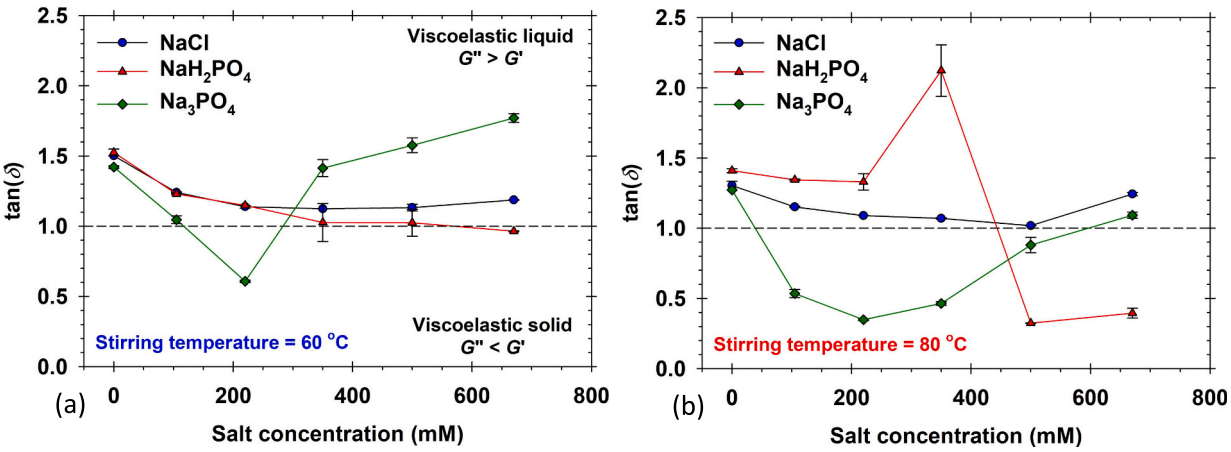

Fig. 3. The effect of salt concentration (NaCl, NaH_2PO_4, Na_3PO_4) on the viscoelastic behavior of the kappa carrageenan solutions, as represented by the loss tangent (tan $\delta = G''/G'$), at stirring temperatures of 60 °C and 80 °C. The dashed line (tan $\delta = 1$) separates the viscoelastic solid regime ($G' > G''$) from the viscoelastic liquid regime ($G'' > G'$).

upon cooling, leading to stronger viscoelastic responses. The resulting network is more elastic, despite originating from coil-rich precursors.

Notably, NaCl exhibited the opposite trend: viscosity decreased when samples were prepared at 80 °C. This suggests that NaCl is ineffective in restructuring of disordered chains into functional networks. It can weakly stabilize interactions when the helices are already partially present (at 60 °C), but does not promote reassembly when starting from a fully disordered coil state. These coions affect the system more strongly, not through direct attractive interactions - which are unlikely due to the electrostatic repulsion between sulfate and phosphate groups - but rather by modulating the local solvent structure, dielectric environment, and steric constraints. Such indirect effects can facilitate the chain rearrangement, enhance the entanglement, and promote junction formations during cooling from the coil state.

For NaH_2PO_4 at 60 °C, the viscosity decreases proportionally to $\dot{\gamma}^{-0.3}$ at 0, 105, and 220 mM. The decrease is monotonic and without inflection points, indicating stable structures with a weak dependence on the deformation. At higher salt concentrations (350, 500, and 650 mM), the viscosity initially follows $\dot{\gamma}^{-0.5}$ up to ~4 s^{-1}, then transitions to $\dot{\gamma}^{-1}$ at higher shear rates. This shift in scaling marks a threshold between distinct structural states of the material.

The inverse power-law region $\eta \propto \dot{\gamma}^{-1}$ observed above $\simeq$10 s^{-1} has an important mechanical implication: because shear stress is defined as $\tau = \eta\dot{\gamma}$, the product of $\dot{\gamma}$ and $\dot{\gamma}^{-1}$ becomes a constant. Hence, once this regime is reached the measured shear stress plateaus and remains essentially independent of further increases in shear rate. Such a flow-stress plateau is a hallmark of weakly connected polymer networks that have been broken down until only viscous drag from solvent-entrained chains resists flow. The onset of this plateau therefore signals complete disruption of carrageenan junction zones and alignment of the residual coil segments with the flow field. Notably, the viscosity of these systems falls in the range of 10 to 1000 Pa·s, typical of viscoelastic fluids rather than highly structured gels. Under these conditions, the flow is governed by bulk deformation, with negligible wall slip, further ensured by the uniform shear field provided by the cone-and-plate geometry.

At 80 °C, NaH_2PO_4 samples follow a similar trend, but the transition from $\dot{\gamma}^{-0.5}$ to $\dot{\gamma}^{-1}$ occurs at lower shear rates, suggesting a less robust structure that is more easily disrupted. Notably, the sample with 500 mM NaH_2PO_4 exhibits an abrupt change in slope near 8 s^{-1}, possibly reflecting a shear-induced network rearrangement or partial collapse of transient junction zones. This localized instability is absent at 670 mM, where the higher ion concentration may promote a more homogeneously entangled and shear-resistant network. Several breakdown mechanisms - such as overscreening of repulsive interactions, junction point destabilization under stress, or intermediate salt-induced structural heterogeneity—could contribute to the observed behavior.

For Na_3PO_4 at 60 °C, the viscosity of solutions at lower salt concentrations (105 and 220 mM) is higher than at higher salt levels (350, 500, 670 mM). At low shear rates, viscosity decreases with a power law of $\sim\dot{\gamma}^{-0.5}$ at all concentrations. A kink appears near 10 s^{-1} for low concentrations, after which the slope shifts to $\dot{\gamma}^{-1}$. At higher concentrations, the transition is smoother and follows $\dot{\gamma}^{-0.3}$.

At 80 °C, Na_3PO_4 samples again show a shift of the kink toward lower shear rates, similar to NaH_2PO_4. This confirms that preparation at higher temperature promotes network formation that is more elastic but also more sensitive to deformations.

The lower apparent viscosity observed for the 220 mM sample at shear rates above 10 s^{-1} may result from a less cohesive or heterogeneously entangled network formed at this intermediate concentration. At this level of ionic strength, the electrostatic screening may be sufficient to partially disrupt interchain repulsion but insufficient to fully promote the stable junction formation, making the network more prone to shear-induced collapse compared to higher concentrations where tighter, more uniform structuring is achieved.

3.1.2. *Oscillatory measurements*

The viscoelastic properties of KC solutions were analyzed through frequency-dependent measurements of the storage (G') and loss (G'') moduli. To improve clarity and prevent overlapping of data in the graphical representations, the curves were shifted by a factor A (Winter & Chambon, 1986). This approach highlights trends across different salt concentrations and preparation conditions without compromising the comparative analysis (Fig. 2). From our experiments, two distinct types of viscoelastic behavior were observed: (1) cases where G' and G'' exhibited similar values, with a crossover point within the measured frequency range, indicating a balance between elastic and viscous components; (2) cases where G' was considerably higher than G'', indicating a predominantly elastic gel-like behavior. These differences reflect the varying degrees of network formation and cross-linking in kappa carrageenan solutions depending on salt types, concentrations, and preparation temperatures.

To supplement the frequency-dependent analysis, the loss tangent $\tan\delta = G''/G'$ was evaluated at $\omega = 1$ Hz (Fig. 3). The dependence of tan δ on ω does not capture the full viscoelastic behavior, but it clearly shows the regions with viscoelastic solid (tan $\delta < 1$, $G' > G''$) and viscoelastic fluid (tan $\delta > 1$, $G' < G''$) rheological behavior. The primary analysis is based on the full G' and G'' frequency spectra shown in Fig. 2.

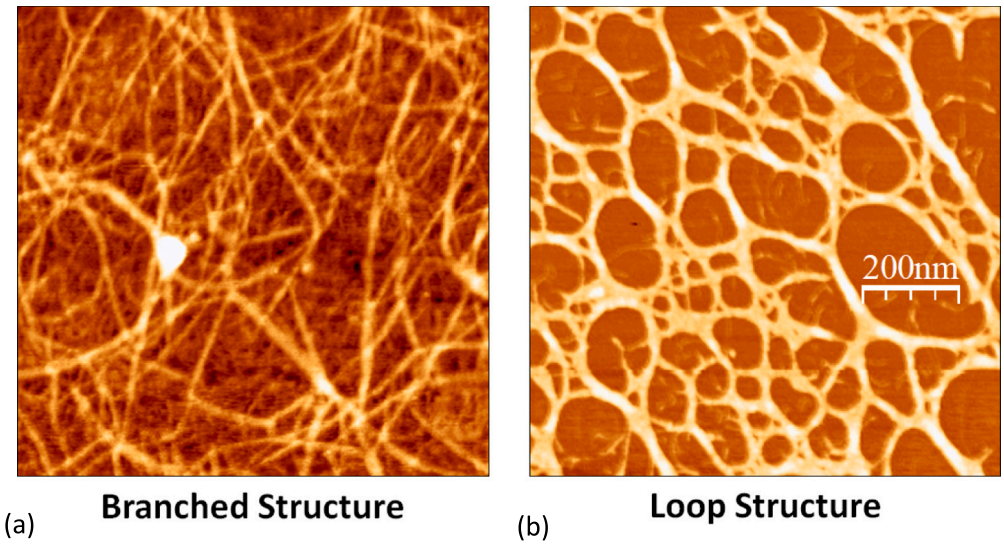

Fig. 4. AFM images of carrageenan networks. (a) Branched structure: multiconnected threads formed by carrageenan helices, creating a complex and intricate network. (b) Loop structure: multiconnected loops, showcasing a network of closed or semi-closed formations. The scale bar in both images is 200 nm.

3.1.2.1. NaCl effects. For solutions containing NaCl, both G′ and G″ increased with frequency, displaying typical viscoelastic behavior (Fig. 2a and b). At both stirring temperatures, the magnitudes of G′ and G″ remained relatively low across all NaCl concentrations (0–670 mM), indicating that NaCl had a limited effect on strengthening the kappa carrageenan network in glycerol. Although G′ was slightly higher than G″, their values were of the same order of magnitude over the measured frequency range. The loss tangent (tan δ at $\omega = 1$ Hz) was close to or above 1, particularly at higher NaCl concentrations and temperatures (Fig. 3, NaCl plots), suggesting that the elastic and viscous components were comparable, with a slight dominance of viscous response. Overall, the presence of NaCl did not significantly enhance gelation under the studied conditions.

3.1.2.2. NaH_2PO_4 effects. The addition of NaH_2PO_4 significantly enhanced the viscoelastic properties of kappa carrageenan solutions. At 60 °C, both *G′* and *G″* increased with rising NaH_2PO_4 concentration, with *G′* consistently exceeding *G″* across the frequency range, indicating a conformational change in the carrageenan network (Fig. 2c). At 80 °C, this effect was further amplified (Fig. 2d), as the elevated temperature promoted the formation of a more robust gel network. This was evidenced by the substantial increase in *G′*, particularly at concentrations above 500 mM. The loss tangent (tan *δ*) values for NaH_2PO_4 solutions at higher concentrations were consistently less than 1, confirming the dominance of elastic over viscous behaviors (Fig. 3, NaH_2PO_4 plots). Thus, NaH_2PO_4 effectively enhances cross-linking and gelation of kappa carrageenan in glycerol, particularly at elevated preparation temperatures (80 °C).

The non-monotonic change in tan *δ* from an increase between 220 and 350 mM, followed by a decrease at 500 mM—suggests a shift from a weakly entangled, viscous-dominated state to a more cohesive, elastic network. At 350 mM, partial structuring may enhance energy dissipation, while at 500 mM, stronger junction formation and chain connectivity increase the storage modulus, reducing tan *δ*. This behavior aligns with the observed transition toward elastic character at higher salt concentrations.

3.1.2.3. Na_3PO_4 effects. The effects of Na_3PO_4 on the viscoelastic properties were similar to those of NaH_2PO_4 but even more pronounced. At 60 °C, both *G'* and *G"* exhibited maximums at intermediate Na_3PO_4 concentrations, indicating the gel formation (Fig. 2e). At 80 °C, the enhancement of *G'* was more considerable and occurred over a wider range of concentrations (Fig. 2f). The highest *G'* values were observed at intermediate Na_3PO_4 concentrations (~220 mM), suggesting an optimal concentration for network formation. At these concentrations and temperatures, the tan *δ* values were consistently well below 1 (Fig. 3, Na_3PO_4 plots), underscoring the highly elastic nature of the gels formed. These results indicate that Na_3PO_4 is particularly effective in promoting the gelation of kappa carrageenan in glycerol, facilitating strong and stable network structures that persist even at elevated temperatures.

3.1.2.4. Overall trends and implications. The oscillatory measurements revealed that the type of coions significantly influences the viscoelastic behavior of kappa carrageenan solutions in glycerol. Phosphate salts (NaH_2PO_4 and Na_3PO_4) were more effective than NaCl in enhancing gel elasticity. This difference is most evident at higher salt concentrations and when samples were prepared at 80 °C. At lower concentrations or at 60 °C, the viscoelastic profiles of NaCl and NaH_2PO_4 appear similar, both showing weak elasticity with tan *δ* values near or slightly above 1. However, NaH_2PO_4 induces a pronounced shift toward elastic behavior at ≥350 mM and 80 °C, as reflected by increased *G′* and reduced tan *δ*. This transition is not observed in NaCl samples, which remain weakly structured across all conditions.

A similar trend is seen for Na_3PO_4: at 60 °C, the rheological response closely resembles that of NaCl except at one intermediate concentration (~220 mM), where moderate elasticity is observed. The strong gelation effect of Na_3PO_4 emerges primarily at 80 °C, where *G′* values increase sharply and tan *δ* drops well below 1, indicating robust network formation. This temperature-dependent enhancement is attributed to the improved dissolution and chain mobility, facilitating stronger ionic interactions and network assembly, particularly for phosphate-containing systems. In contrast, NaCl does not show such improvement with temperature, highlighting its limited ability to support network formation under these conditions.

The loss tangent (tan *δ*) provided additional insight into the viscoelastic nature of the gels (Fig. 3). For phosphate salts at optimal concentrations and higher temperatures, tan *δ* values were significantly less than 1, confirming the formation of strong, elastic gels suitable for applications requiring structural integrity. In contrast, NaCl solutions exhibited tan *δ* values around or above 1, suggesting limited gelation and predominance of viscoelastic fluid behavior.

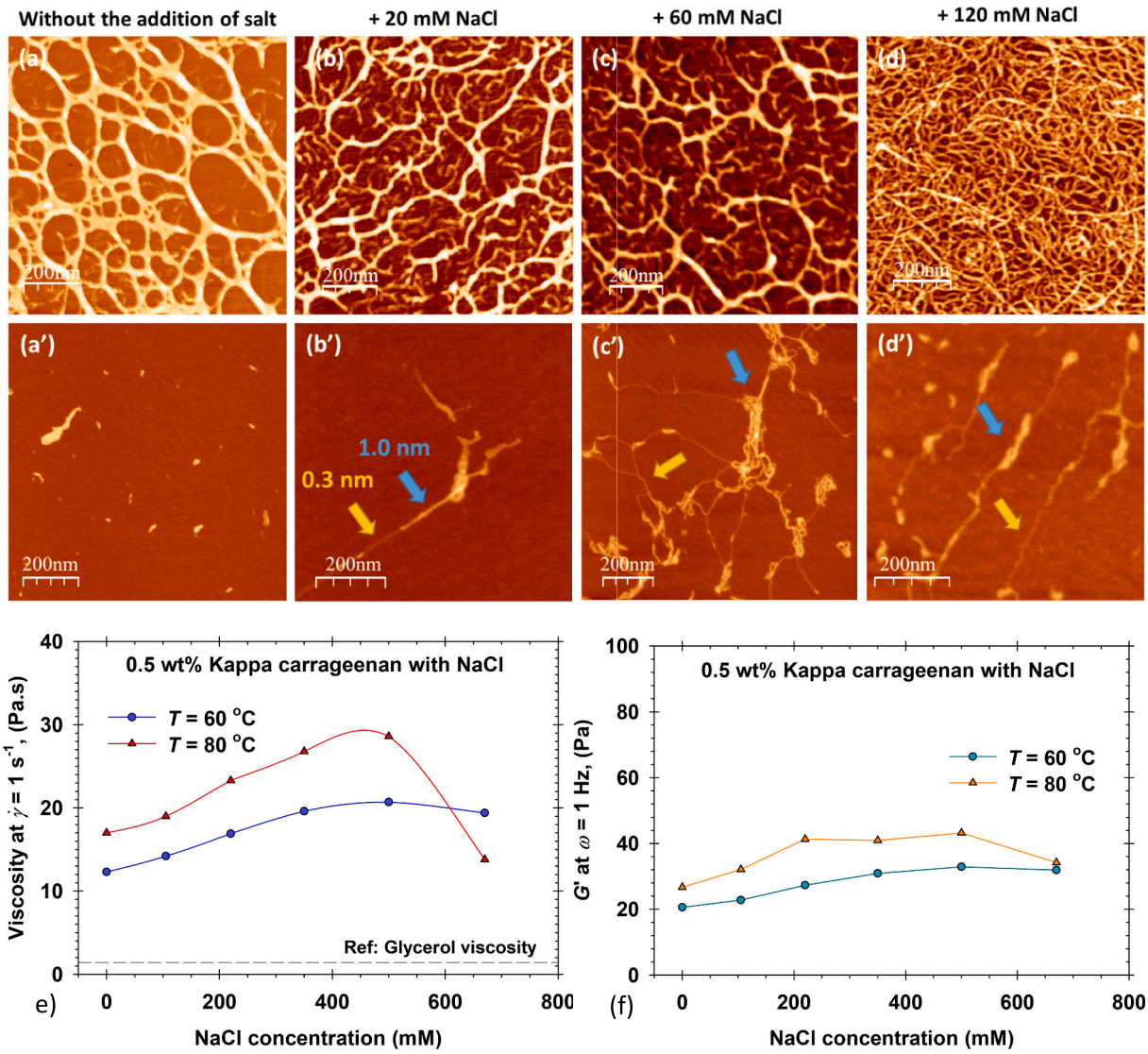

Fig. 5. Impact of NaCl on kappa carrageenan properties at different temperatures. AFM images of 0.1 wt% kappa carrageenan networks formed in the presence of varying concentrations of NaCl at (a) without NaCl, (b) 20 mM, (c) 60 mM, and (d) 120 mM NaCl, after stirring at 60 °C (top row) and 80 °C (bottom row). (e): Viscosity of 0.5 wt% kappa carrageenan solutions with NaCl as a function of NaCl concentration at 60 °C and 80 °C. (f) Storage modulus (G') of 0.5 wt% kappa carrageenan solutions with NaCl at a frequency of 1 Hz, at 60 °C and 80 °C.

3.2. AFM measurements of kappa carrageenan structures

The AFM results for immobilized kappa carrageenan structures from glycerol solutions on modified mica substrates closely resemble those obtained from aqueous solutions (Chen et al., 2019; Funami et al., 2007; Ikeda et al., 2001; Schefer et al., 2015; Sokolova et al., 2013; Walther et al., 2006). Depending on the conditions, typical helical or coiled structures were observed, confirming that glycerol does not introduce any unexpected features into the system. Consequently, we adopt the nomenclature established by Mezzenga's group for primary, secondary, and higher-order helical structures (Diener et al., 2019) and further introduce the terms “branched” and “loop” structures to describe additional carrageenan network morphologies observed under certain experimental conditions (see Fig. 4).

Building on these observations, one can define two distinct structural formations in the AFM images: the branched structure and the loop structure. The branched structure is characterized by multiconnected threads formed through the helical arrangement of carrageenan polysaccharide chains, resulting in a complex network that enhances the overall mechanical strength and stability. In contrast, the loop structure consists of interconnected loops, where the carrageenan chains bend and intertwine to form closed or semi-closed formations that contribute to the network's flexibility and resilience. Both structures are critical for understanding the properties and behavior of carrageenan in various applications.

While AFM provides valuable nanoscale insight, it cannot fully capture the complexity of the three-dimensional gel network or predict bulk rheological behavior directly. Features such as helix thickness (reflecting helical order), junction point density, and chain rigidity or flexibility offer qualitative cues that align with observed viscoelastic responses. However, these are two-dimensional projections of surface-adsorbed structures, and therefore cannot reflect dynamic interactions, entanglement, or crosslinking in the bulk phase. To build a predictive structure-rheology relationship, additional multiscale characterization would be necessary. This study aims only to highlight how specific coions and preparation temperatures affect the carrageenan network at the nanoscale and how these trends qualitatively support the rheological results.

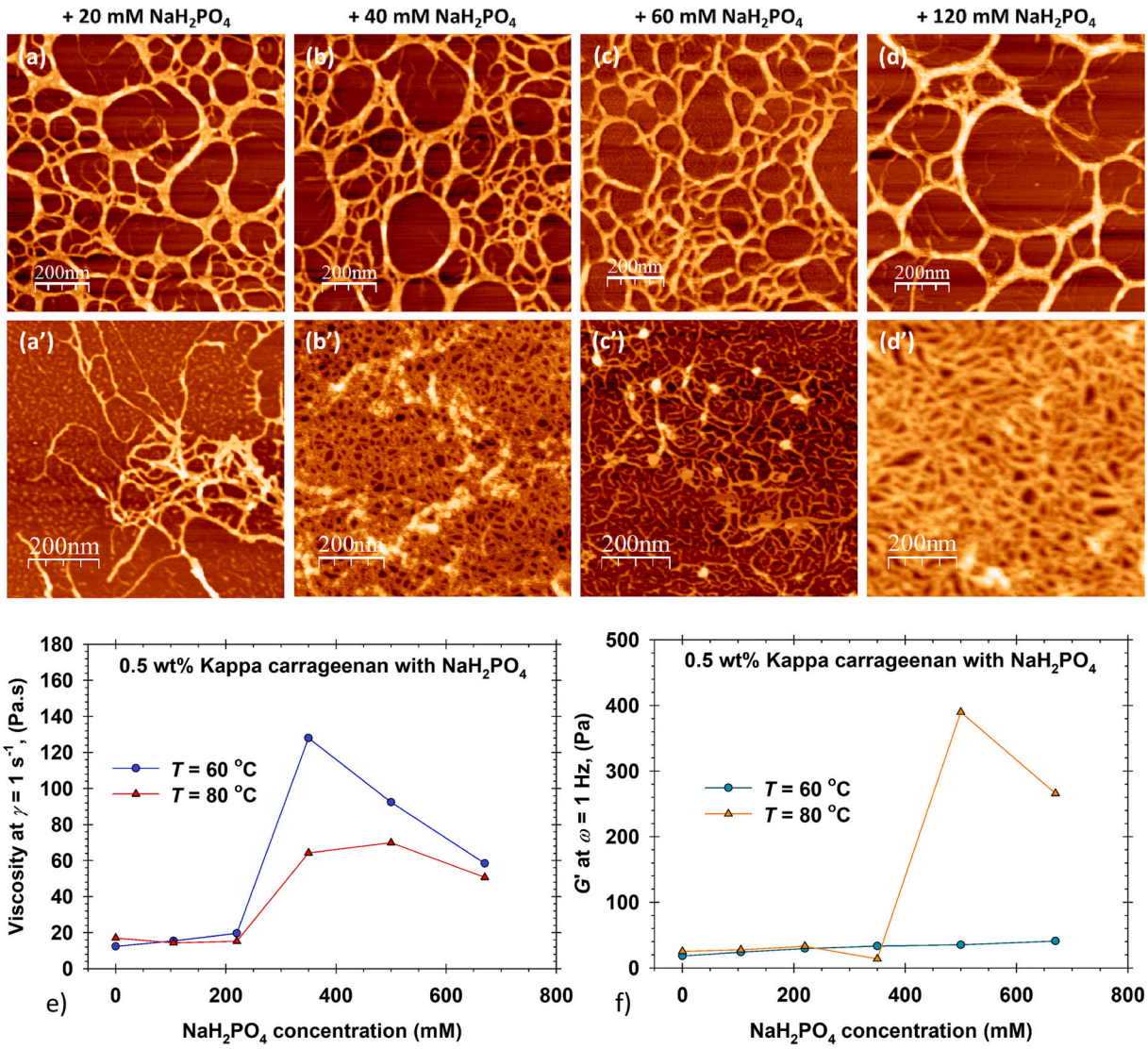

Fig. 6. Impact of NaH_2PO_4 on kappa carrageenan properties at different temperatures. AFM images of 0.1 wt% kappa carrageenan networks formed in the presence of varying concentrations of NaH_2PO_4 at (a) 20 mM, (b) 40 mM, (c) 60 mM, and (d) 120 mM NaH_2PO_4, after stirring at 60 °C (top row) and 80 °C (bottom row). (e): Viscosity of 0.5 wt% kappa carrageenan solutions with NaH_2PO_4 as a function of NaH_2PO_4 concentration at 60 °C and 80 °C. (f) Storage modulus (*G'*) of 0.5 wt% kappa carrageenan solutions with NaH_2PO_4 at a frequency of 1 Hz, at 60 °C and 80 °C.

3.2.1. *NaCl effect*

The results obtained at 60 °C in the absence of added NaCl show a clearly defined multiconnected loop structure (Fig. 5a). The thickness of the strands ranges between 2 and 4 nm, indicating a network structure composed of highly ordered helices. At this temperature, kappa carrageenan in glycerol does not undergo the helix-to-coil transition (Ramakrishnan & Prud'homme, 2000b). However, it reconfigures into a highly interconnected structure with significant viscosity and elasticity. It is important to note that the AFM results are obtained at a carrageenan concentration of 0.1 wt%, whereas the rheological measurements are performed at a concentration of 0.5 wt%. The reduction in concentration for the AFM experiments is due to the experimental observation that higher concentrations than 0.1 wt% did not yield reliable images. The AFM images provide a 2D projection of the carrageenan structures adsorbed onto a mica surface at 0.1 wt% concentration. While these immobilized structures reflect conformations present in the bulk solution, they do not capture the full 3D network topology. As such, the AFM results are interpreted qualitatively as representative of nanoscale organization, and are correlated with rheological behavior, without implying direct structural equivalence to the bulk gel.

With the addition of NaCl, the multiconnected loops in the network unravel (Fig. 5b and c), and at the highest concentration (120 mM, Fig. 5d), an intertwined carrageenan strand state is observed. This restructuring leads to a slight increase in both viscosity and elasticity. At 80 °C, where the helix-to-coil transition occurs, the addition of NaCl results in carrageenan adopting a coil conformation. NaCl effectively interacts and influences both inter- and intramolecular structural factors. As a result, the AFM measurements reveal coil elements with a thickness of 0.3 nm, as well as the formation of primary (yellow arrows) and secondary (blue arrows) helical structures (Fig. 5 b'-d').

What is noticeable is that the viscosity achieved when stirred at 80 °C is 1.4 times higher than that at 60 °C until the addition of 500 mM NaCl (Fig. 5e). Beyond this concentration, the viscosity decreases in both series, but the decrease is much more pronounced in the series stirred at 80 °C. Elasticity follows a similar trend to that of viscosity, where the system stirred at 80 °C consistently exhibits approximately 1.4 times higher elasticity (Fig. 5f).

3.2.2. *NaH_2PO_4 effect*

Fig. 6 shows the AFM images illustrating the evolution of kappa

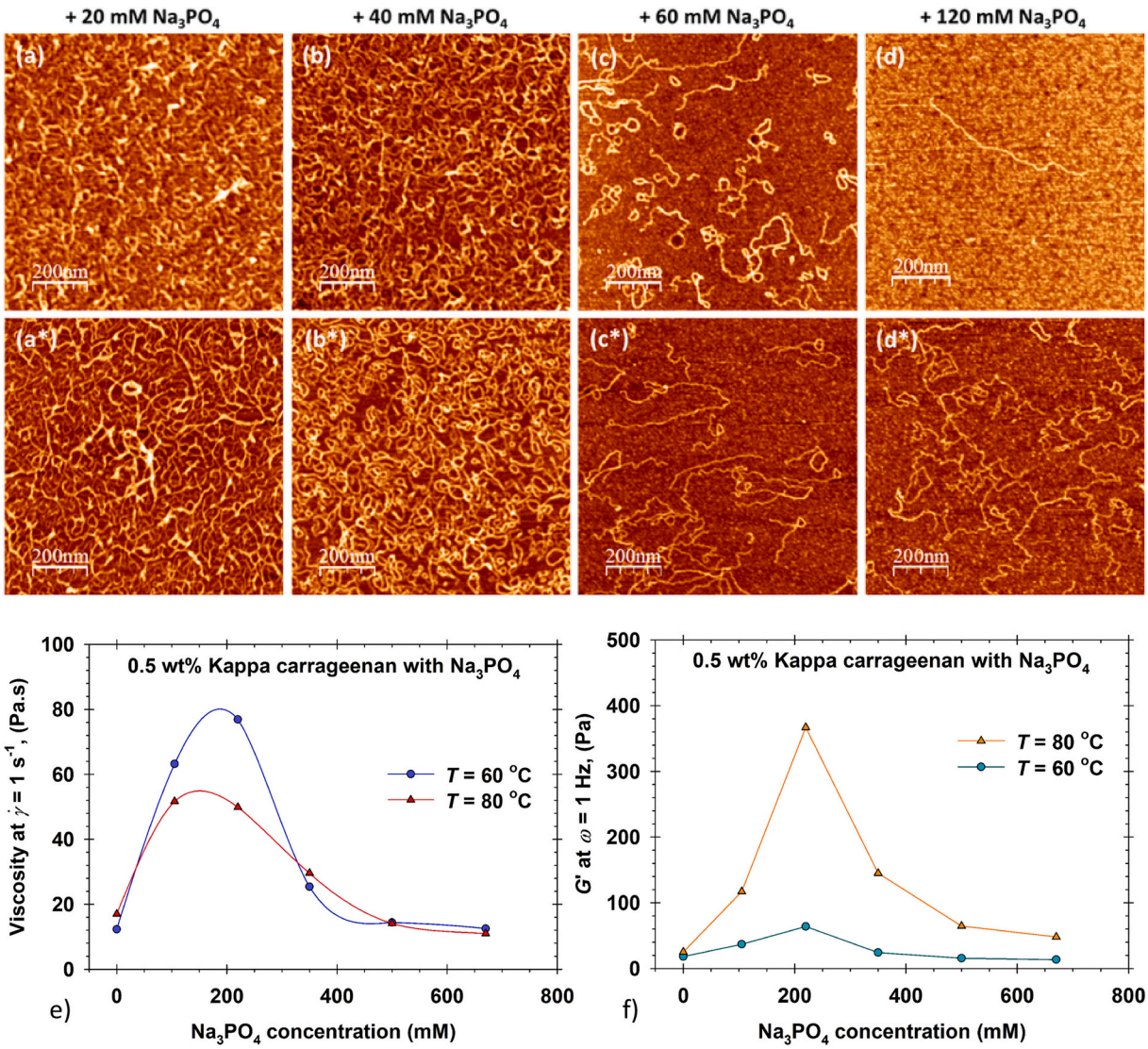

Fig. 7. Impact of Na_3PO_4 on kappa carrageenan properties at different temperatures. AFM images of 0.1 wt% kappa carrageenan networks formed in the presence of varying concentrations of Na_3PO_4 at (a) 20 mM, (b) 40 mM, (c) 60 mM, and (d) 120 mM Na_3PO_4, after stirring at 60 °C (top row) and 80 °C (bottom row). (e): Viscosity of 0.5 wt% kappa carrageenan solutions with Na_3PO_4 as a function of Na_3PO_4 concentration at 60 °C and 80 °C. (f) Storage modulus (G') of 0.5 wt% kappa carrageenan solutions with Na_3PO_4 at a frequency of 1 Hz, at 60 °C and 80 °C.

carrageenan network structures with varying concentrations of NaH_2PO_4 and the effects of different stirring temperatures.

At a stirring temperature of 60 °C, kappa carrageenan forms a multiconnected loop network, which retains its integrity even as the concentration of NaH_2PO_4 increases. In terms of viscosity, this series demonstrates a sharp increase when the NaH_2PO_4 concentration exceeds 200 mM, followed by a gradual decline. The salt concentration does not affect the measured elasticities, indicating that the multiconnected loop network inherently exhibits low elasticity. The observed increase in the apparent viscosity might be attributed to the formation of higher-order helices, which increase the yield stress of the system and thereby affect the viscosity measurements. This effect is not reflected in the dynamic oscillation experiments used to determine the system's elasticity.

In contrast, the experiments conducted at 80 °C reveal fundamentally different structures compared to those at 60 °C. At lower concentrations of NaH_2PO_4, partial network entanglement of carrageenan is observed, along with numerous discrete components. For the sample containing 40 mM NaH_2PO_4 and 0.1 wt% kappa carrageenan, a network structure featuring "hairpin" inclusions is observed. These inclusions are known to contribute to the higher viscosities and elasticities. At 120 mM NaH_2PO_4, a well-formed network of multiconnected threads with a thickness of approximately 4 nm is observed, indicating the significant impact of NaH_2PO_4 concentration on the structure of kappa carrageenan, dependent on the stirring temperature.

3.2.3. *Na_3PO_4 effect*

The results obtained from AFM clearly show that even a small addition of Na_3PO_4 leads to significant changes in the structuring of kappa carrageenan in glycerol (Fig. 7). A key difference to note is that at a temperature of 60 °C, prior to the helix-to-coil transition, the multiconnected network is not observed. Instead, segmented short carrageenan strands are seen, overlapping but weakly connected. With increasing Na_3PO_4 concentration, it becomes evident that less kappa carrageenan adheres to the mica surface. The immobilization procedure is based on ionic interactions, suggesting that this effect may be due to charge screening as the concentration of Na_3PO_4 increases.

The AFM results at 80 °C follows the same trend. However, at lower concentrations (20 and 40 mM Na_3PO_4), the carrageenan appears to form a structure with more junction points compared to at 60 °C. At the highest investigated salt concentration of 120 mM, carrageenan is

observed in a primary coil state. Thus, the degree of carrageenan aggregation decreases with increasing Na_3PO_4 concentration.

The rheological behavior of both systems is similar. Both viscosity and elasticity reach a maximum at around 200 mM. Interestingly, the viscosity curves at 60 °C show higher viscosity, while in terms of elasticity, the effect is opposite, with the system at 80 °C exhibiting higher elasticity.

4. Conclusions

This study provides valuable insights into the conformational and rheological behavior of kappa carrageenan in glycerol, with a focus on the effect of coions coming from sodium salts (NaCl, NaH_2PO_4, Na_3PO_4) and the preparation temperature (60 °C and 80 °C). Using a combination of rheological analysis and AFM, we revealed most important trends in gelation, network formation, and viscoelastic properties.

1. Effect of Salt Type and Concentration: The type of sodium salt plays a pivotal role in modulating the structural and viscoelastic properties of kappa carrageenan in glycerol. NaCl primarily disrupted the network, resulting in less robust structures and predominantly viscous behavior, as reflected by tan δ values around or above 1. In contrast, NaH_2PO_4 and Na_3PO_4 enhanced gelation, promoting the formation of dense, branched networks with significantly higher elastic moduli (G') and tan δ values consistently below 1, particularly at intermediate salt concentrations (~220–350 mM).
2. Effect of Temperature: Preparation temperature profoundly influenced the self-assembly of kappa carrageenan. At 60 °C, the networks were dominated by loop structures at low salt concentrations and transitioned to denser, branched formations with increasing salt concentration. At 80 °C, the elevated temperature facilitated stronger cross-linking for phosphate salts (NaH_2PO_4 and Na_3PO_4), resulting in more robust networks and enhanced gel elasticity. However, NaCl solutions showed reduced structural integrity at higher temperatures due to the helix-to-coil transition.
3. Salt-Specific Behavior: Among the salts studied, Na_3PO_4 exhibited the most pronounced effects, forming the densest and the most elastic networks. The AFM images and rheological data consistently highlighted Na_3PO_4's superior ability to promote gelation and structural integrity, even at elevated temperatures. This makes Na_3PO_4 particularly suitable for applications requiring strong and stable gels.
4. Practical Implications: The findings underscore the importance of selecting appropriate salt types, concentrations, and preparation conditions to tailor the viscoelastic properties of kappa carrageenan gels. These insights are highly relevant for applications in cosmetic, food, pharmaceutical, and biotechnological industries, where the ability to modulate gel strength and elasticity is critical.

By combining structural (AFM) and mechanical (rheological) analyses, this study provides a comprehensive understanding of kappa carrageenan's behavior in non-aqueous systems, paving the way for the development of novel materials with customizable properties. While AFM and rheological measurements were conducted at different total polymer concentrations due to methodological constraints, the polymer-to-salt ratio was maintained, ensuring consistent structural context. The study focuses on a defined concentration range and a selected set of coions, which provides a controlled framework for analysis. Future work could extend these findings by examining a broader range of conditions and applying complementary structural techniques.

CRediT authorship contribution statement

Mihail T. Georgiev: Writing – review & editing, Writing – original draft, Visualization, Methodology, Formal analysis, Data curation, Conceptualization. **Silviya S. Simeonova:** Methodology, Investigation, Data curation. **Boris G. Konstantinov:** Investigation. **Krassimir D. Danov:** Writing – review & editing, Supervision, Project administration, Conceptualization. **Robert Riley:** Resources, Funding acquisition, Conceptualization. **Dawn Woodall:** Resources, Funding acquisition, Conceptualization.

Funding

This work was partially supported by Unilever R&D Port Sunlight, UK.

Declaration of competing interest

The authors declare that they have no known competing financial interests or personal relationships that could have appeared to influence the work reported in this paper.

Acknowledgments

The authors are grateful to the European Regional Development Fund under the Operational Program "Scientific Research, Innovation and Digitization for Smart Transformation 2021-2027", Project CoC "Smart Mechatronics, Eco- and Energy Saving Systems and Technologies", BG16RFPR002-1.014-0005.

Data availability

Data will be made available on request.

References

Brenner, T., Tuvikene, R., Parker, A., Matsukawa, S., & Nishinari, K. (2014). Rheology and structure of mixed kappa-carrageenan/iota-carrageenan gels. *Food Hydrocolloids, 39*, 272–279. https://doi.org/10.1016/j.foodhyd.2014.01.024

Bui, V. T. N. T., Nguyen, B. T., Renou, F., & Nicolai, T. (2019). Rheology and microstructure of mixtures of iota and kappa-carrageenan. *Food Hydrocolloids, 89*, 180–187. https://doi.org/10.1016/j.foodhyd.2018.10.034

Cao, Y., & Mezzenga, R. (2020). Design principles of food gels. *Nature Food, 1*(2), 106–118. https://doi.org/10.1038/s43016-019-0009-x

Chen, J., Chen, W., Duan, F., Tang, Q., Li, X., Zeng, L., Zhang, J., Xing, Z., Dong, Y., Jia, L., & Gao, H. (2019). The synergistic gelation of okra polysaccharides with kappa-carrageenan and its influence on gel rheology, texture behaviour and microstructures. *Food Hydrocolloids, 87*, 425–435. https://doi.org/10.1016/j.foodhyd.2018.08.003

Ciancia, M., Milas, M., & Rinaudo, M. (1997). On the specific role of coions and counterions on κ-carrageenan conformation. *International Journal of Biological Macromolecules, 20*(1), 35–41. https://doi.org/10.1016/S0141-8130(97)01149-5

Derkach, S. R., Voron'ko, N. G., Kuchina, Y. A., Kolotova, D. S., Gordeeva, A. M., Faizullin, D. A., … Makshakova, O. N. (2018). Molecular structure and properties of κ-carrageenan-gelatin gels. *Carbohydrate Polymers, 197*, 66–74. https://doi.org/10.1016/j.carbpol.2018.05.063

Diener, M., Adamcik, J., Sánchez-Ferrer, A., Jaedig, F., Schefer, L., & Mezzenga, R. (2019). Primary, secondary, tertiary and quaternary structure levels in linear polysaccharides: From random coil, to single Helix to supramolecular assembly. *Biomacromolecules, 20*(4), 1731–1739. https://doi.org/10.1021/acs.biomac.9b00087

Funami, T., Hiroe, M., Noda, S., Asai, I., Ikeda, S., & Nishinari, K. (2007). Influence of molecular structure imaged with atomic force microscopy on the rheological behavior of carrageenan aqueous systems in the presence or absence of cations. *Food Hydrocolloids, 21*(4), 617–629. https://doi.org/10.1016/j.foodhyd.2006.07.013

Geonzon, L. C., Bacabac, R. G., & Matsukawa, S. (2019). Network structure and gelation mechanism of kappa and iota carrageenan elucidated by multiple particle tracking. *Food Hydrocolloids, 92*, 173–180. https://doi.org/10.1016/j.foodhyd.2019.01.062

Hermansson, A.-M. (1989). Rheological and microstructural evidence for transient states during gelation of kappa-carrageenan in the presence of potassium. *Carbohydrate Polymers, 10*.

Hjerde, T., Smidsrød, O., & Christensen, B. E. (1999). Analysis of the conformational properties of κ- and ι-carrageenan by size-exclusion chromatography combined with low-angle laser light scattering. *Biopolymers, 49*(1), 71–80. https://doi.org/10.1002/(SICI)1097-0282(199901)49:1<71::AID-BIP7>3.0.CO;2-H

Ikeda, S., Morris, V. J., & Nishinari, K. (2001). Microstructure of aggregated and nonaggregated κ-carrageenan helices visualized by atomic force microscopy. *Biomacromolecules, 2*(4), 1331–1337. https://doi.org/10.1021/bm015610l

Mangione, M. R., Giacomazza, D., Bulone, D., Martorana, V., Cavallaro, G., & San Biagio, P. L. (2005). K + and Na + effects on the gelation properties of κ-carrageenan. *Biophysical Chemistry, 113*(2), 129–135. https://doi.org/10.1016/j.bpc.2004.08.005

Mangione, M. R., Giacomazza, D., Bulone, D., Martorana, V., & San Biagio, P. L. (2003). Thermoreversible gelation of κ-carrageenan: Relation between conformational transition and aggregation. *Biophysical Chemistry, 104*(1), 95–105. https://doi.org/10.1016/S0301-4622(02)00341-1

Ramakrishnan, S., & Prud'homme, R. K. (2000a). Behavior of κ-carrageenan in glycerol and sorbitol solutions. *Carbohydrate Polymers, 43*(4), 327–332. https://doi.org/10.1016/S0144-8617(00)00177-6

Ramakrishnan, S., & Prud'homme, R. K. (2000b). Effect of solvent quality and ions on the rheology and gelation of κ-carrageenan. *Journal of Rheology, 44*(4), 885–896. https://doi.org/10.1122/1.551119

Ramm, I., Sanchez-Fernandez, A., Choi, J., Lang, C., Fransson, J., Schagerlöf, H., Wahlgren, M., & Nilsson, L. (2021). The impact of glycerol on an affibody conformation and its correlation to chemical degradation. *Pharmaceutics, 13*(11). https://doi.org/10.3390/pharmaceutics13111853

Rupert, R., Rodrigues, K. F., Thien, V. Y., & Yong, W. T. L. (2022). Carrageenan from *Kappaphycus alvarezii* (Rhodophyta, Solieriaceae): Metabolism, structure, production, and application. *Frontiers in Plant Science, 13*. https://doi.org/10.3389/fpls.2022.859635

Schefer, L., Adamcik, J., & Mezzenga, R. (2014). Unravelling secondary structure changes on individual anionic polysaccharide chains by atomic force microscopy. *Angewandte Chemie, International Edition, 53*(21), 5376–5379. https://doi.org/10.1002/anie.201402855

Schefer, L., Usov, I., & Mezzenga, R. (2015). Anomalous stiffening and ion-induced coil-Helix transition of Carrageenans under monovalent salt conditions. *Biomacromolecules, 16*(3), 985–991. https://doi.org/10.1021/bm501874k

Sokolova, E. V., Chusovitin, E. A., Barabanova, A. O., Balagan, S. A., Galkin, N. G., & Yermak, I. M. (2013). Atomic force microscopy imaging of carrageenans from red algae of Gigartinaceae and Tichocarpaceae families. *Carbohydrate Polymers, 93*(2), 458–465. https://doi.org/10.1016/j.carbpol.2012.12.026

Stenner, R., Matubayasi, N., & Shimizu, S. (2016). Gelation of carrageenan: Effects of sugars and polyols. *Food Hydrocolloids, 54*, 284–292. https://doi.org/10.1016/j.foodhyd.2015.10.007

Tako, M. (2015). The principle of polysaccharide gels. *Advances in Bioscience and Biotechnology, 06*(01), 22–36. https://doi.org/10.4236/abb.2015.61004

Thrimawithana, T. R., Young, S., Dunstan, D. E., & Alany, R. G. (2010). Texture and rheological characterization of kappa and iota carrageenan in the presence of counter ions. *Carbohydrate Polymers, 82*(1), 69–77. https://doi.org/10.1016/j.carbpol.2010.04.024

Walther, B., Lorén, N., Nydén, M., & Hermansson, A. M. (2006). Influence of κ-carrageenan gel structures on the diffusion of probe molecules determined by transmission electron microscopy and NMR diffusometry. *Langmuir, 22*(19), 8221–8228. https://doi.org/10.1021/la061348w

Watase, M., Nishinari, K., Williams, P. A., & Phillips, G. O. (1990). Effect of ammonium salts on rheological and thermal properties of kappa-carrageenan gels. *Food Hydrocolloids, 4*(3), 227–237. https://doi.org/10.1016/S0268-005X(09)80156-2

Winter, H. H., & Chambon, F. (1986). Analysis of linear viscoelasticity of a crosslinking polymer at the gel point. *Journal of Rheology, 30*(2), 367–382. https://doi.org/10.1122/1.549853